

OTKA final report K68140

Investigation of zinc containing solution and surface

Results on surface chemistry

Heterogeneous catalysis is the work horse in the chemical industry. Therefore, research into a deeper understanding of catalytic processes has a long history. Currently rising oil prices and climate change issues have led to a renewed interest in two heterogeneous catalytic reactions. One is the hydrogenation of carbon monoxide and carbon dioxide to form methanol. This reaction is also known as the Fischer Tropsch process and it enables the production of petrochemical products from coal.

The other is the reverse reaction, the dehydrogenation of methanol to form hydrogen and CO₂. The hydrogen can then be used in a fuel cell to generate electricity. When the methanol is produced from biomass this would be a way to avoid carbon dioxide emissions, as the CO₂ from the dehydrogenation of methanol is recycled in plant growth. Palladium [e.g. ⁱ, ⁱⁱ, ⁱⁱⁱ, ^{iv}, ^v, ^{vi}] and rhodium [e.g. ^{vii}, ^{viii}, ^{ix}, ^x, ^{xi}, ^{xii}, ^{xiii}] were studied recently for their activity in the dehydrogenation of methanol. From these studies it is quite clear that the single metals are not the best choice as catalysts for these reactions. Catalytic studies have shown that Pd – ZnO catalysts show a high activity for the dehydrogenation of methanol [e.g. ^{xiv}, ^{xv}, ^{xvi}, ^{xvii}]. At the same time these systems can also be used to catalyze the hydrogenation of CO and CO₂ to form methanol [e.g. ^{xviii}, ^{xix}]. Another promising system for methanol synthesis is the Cu – ZnO system, which has been studied in more detail by several groups [e.g. ^{xx}, ^{xxi}, ^{xxii}, ^{xxiii}, ^{xxiv}].

For the Pd/ZnO and Cu/ZnO systems the main research focus so far has been on actual catalysts for methanol steam reforming. It has been shown that partial Pd – Zn alloy formation occurs, combined with an increased selectivity towards CO₂ [^{xiv}, ^{xvi}, ^{xvii}]. The reverse reaction, the formation of methanol from CO₂, also is facilitated by the formation of Pd – Zn alloy on Pd/ZnO catalysts according to references [^{xviii}, ^{xix}]. In the moment there seems to be a lack of more basic surface science studies of these systems. Only a few studies on the basic science of the Pd – Zn system do exist in form of theoretical studies [^{xxv}, ^{xxvi}, ^{xxvii}].

The main idea of the proposed research is the connection of surface science investigations of Pd(111) – Zn and Pd(111) – ZnO and Cu(110) surfaces using reflection absorption infrared spectroscopy (RAIRS), thermal desorption spectroscopy (TDS) and scanning tunneling microscopy (STM) with high pressure kinetic measurements (CO and CO₂ hydrogenation and methanol dehydrogenation) on the same surfaces, which are always prepared in the same way under UHV conditions prior to analysis or high pressure reactions.

In order to get more detailed insight on the species to characterise the adsorption geometry and energy and the IR spectra of CO, methanol and all possible intermediates at the single crystal surfaces, we performed theoretical calculation too. In addition, it is of the utmost importance to calculate not only structures, but also STM images using a DFT approach, in order to delineate the detailed structure of the surface alloys and oxide films.

All adsorption energies as well as the electronic and vibrational properties were calculated using the Vienna Ab Initio Simulation Package (VASP)^{xxviii, xxix}, which is a density functional theory (DFT) code with a plane wave basis set

1.

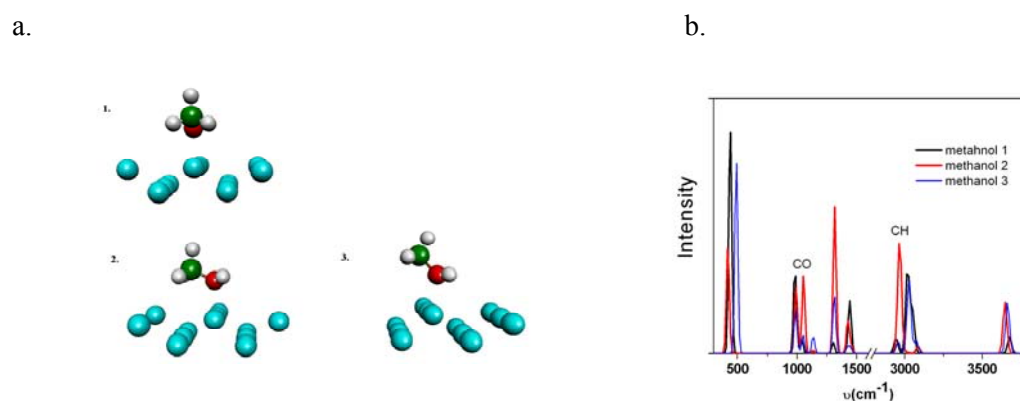
The adsorption and reaction of methanol on Cu(110) and on an oxygen stripe phase on Cu(110) was studied using RAIRS, TPD and DFT. RAIRS measurements show very similar spectra for a monolayer of methanol with and without preadsorbed oxygen. DFT calculations showed that this is due to the fact that one cannot distinguish adsorbed methanol and methoxy adsorbed on the more stable short bridge site by looking at the ν -CO frequency. The formation of carbon dioxide during thermal desorption seems to take place via a previously unknown η -formaldehyde and OH intermediate on the surface that was detected in temperature programmed RAIRS experiments and characterized by DFT.

With coadsorbed oxygen the reaction products are formaldehyde, H₂ and CO₂. DFT and RAIRS results suggest that the intermediate leading to CO₂ is an η_2 -formaldehyde and OH species on the surface, rather than formate.

I presented here three most stable structures according to DFT for single methanol molecules on the Cu(110) surface which are shown in figure 1 a. In all of these structures the methanol adsorbs via the oxygen atom and the methyl group is tilted towards the surface. The corresponding calculated IR spectra are shown in figure 1b

Figure 1:

a.) Side view of the three stable geometries of methanol molecules on Cu(110) (see Table I for details). Cu atoms are blue, carbon is green, oxygen red and hydrogen light grey. b. Calculated IR spectra of the three geometries shown in (a). The positions of the CO vibrations and CH vibrations are indicated in the spectrum.



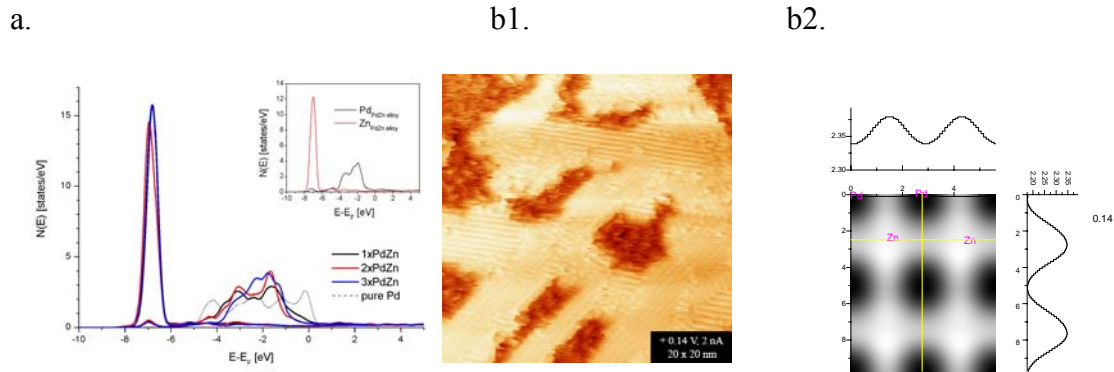
1. Singnurkar, P., **Bako, I.**, Koch, H. P., Demirci, E., Winkler, A., Schennach, R.: DFT and RAIRS investigations of methanol on Cu(110) and on oxygen-modified Cu(110), J. Phys. Chem. C, 2008, 112(36), 14034

2.

DFT calculations have confirmed that a 2 ML (2x1)-PdZn surface alloy on the Pd substrate is more stable than 1 ML due to the minimization of the surface energy . DFT calculations have predicted that the PdZn bilayers are energetically more stable than single PdZn layers and have established their structural parameters . The results of the density of states (DOS) calculation have demonstrated that with increasing Zn adsorption on the PdZn the Zn is approximating pure Zn. We showed a significant charge transfer from Zn to Pd using Bader analyses.

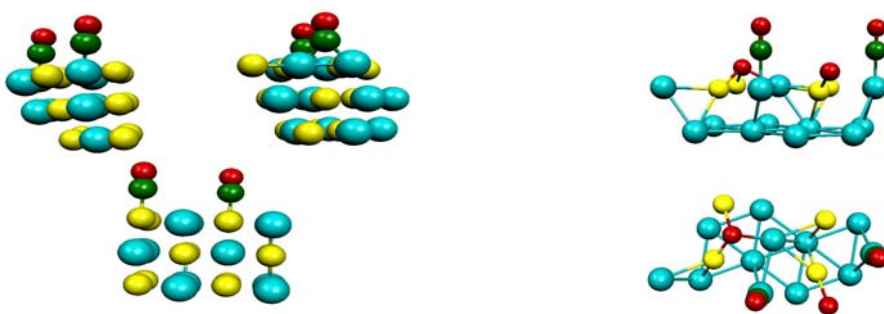
Figure 2.

a. Calculated local density of states (LDOS) of different amounts of PdZn layers on a Pd substrate., b. The measured(b1) and simulated(b2) STM images of one ML PdZn on the Pd substrate



We performed theoretical calculation on different CO coverage on Pd(111) and Pd(111)-Zn systems. We also calculated the vibrational frequencies of CO on different surfaces, which results can help to interpret to the experimentalist the IR spectra, and create a possible structural model of investigated system. We showed that the adsorption energy of CO molecule is decreasing as function of Zn in the first layer. We prove the existence of surface alloy film formation too.

Figure 3. The investigated adsorbed CO and O+CO structure on PdZn surface layer .



3.

The adsorption of small molecules (methanol, formaldehyde, methoxy, carbon monoxide and water) on a (2x1) PdZn and PdZnO surface alloy on Pd(111) has been studied using DFT calculations. The results have shown that methanol is only weakly bound on the surface. Also the differences of the adsorption energies between the different adsorption sites are so small, that one can conclude that methanol is very mobile on the surface. For comparison the adsorption energy of methoxy is nearly ten times larger than that of methanol. The adsorption energy only increases with higher methanol coverages, where chain structures with hydrogen bonds between the methanol molecules are formed. The highest adsorption energy was found for the formate species followed by the methoxy species. The formaldehyde species shows quite some electronic interaction with the surface, however the stable η_2 formaldehyde has only an adsorption energy of about 0.49 eV. The calculated IR spectra of the different species fit quite well to the experimental values available in the literature

1. Weirum, G., Kratzer, M., Koch, H. P., Tamtogl, A., Killmann, J., **Bako, I.**, Winkler, A., Surnev, S., Netzer, F. P., Schennach, R.: Growth and desorption kinetics of ultrathin Zn layers on Pd(111), *J. Phys. Chem. C* 2009, 113(22), 9788
2. Koch HP, **Bako I**, Schennach R Adsorption of small molecules on a (2 x 1) PdZn surface alloy on Pd(111) : *Surface Science* 2010,604, 596
3. Koch, H.P. **Bako. I.** , Weirum, G Kratzer M, Schennach R A theoretical study of Zn adsorption and desorption on a Pd(111) substrate *Surface Science* 2010,604 926

Results concerning to the liquid structure

4.

Simulation molecular dynamics and Car-Parrinello and diffraction x-ray and neutron studies on nitromethane are compared aiming at the determination of the liquid structure. It is well known that in the gas phase the rotation of the CH₃ group is nearly free and in the solid state there is a barrier of 0.6–0.86 kcal/mol between the two conformers of the nitromethane molecule. We showed analyzing the CPMD trajectories that the rotation of CH₃ group is free in the liquid phase.

For the studied liquid, the diffraction methods are performing very well in the determination of intramolecular structure, but they do not give detailed structural information on the intermolecular structure. The good agreement between the diffraction experiments and

the results of molecular dynamics simulations justifies the use of simulations for the more detailed description of the liquid structure using partial radial distribution functions and orientational correlation functions. Liquid nitromethane is described as a molecular liquid without strong intermolecular interactions such as hydrogen bonding, but with detectable orientational correlations resulting in preferential antiparallel order of the neighboring molecules

5.

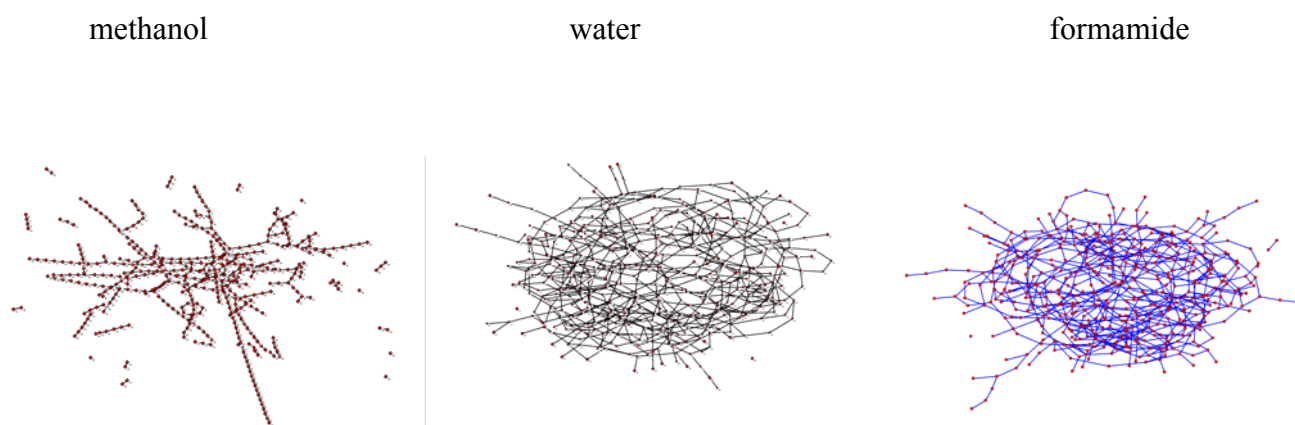
In general hydrogen-bond network plays an important role in determining the physical properties of several molecular liquids and solids. Among these, water is the most extensively studied material because of its simple molecular constitution and high importance. In addition, water is one of the most common polar solvents in synthetic chemistry. The power of liquid water as a solvent and many of its unusual properties are often attributed to its strong hydrogen-bonded network. Hydrogen-bonding interactions also exist in other classes of chemical compounds leading to linear chains or cyclic associations of molecules, carboxylic acids or alcohols for example. The structure of these complex networks can be characterized by their topological properties. The topological properties of the hydrogen-bonded structure of liquid water have been analyzed several times in the past 20 years. It became clear from our analysis that the formamide molecules - similarly to water - are forming a percolating hydrogen-bonded network

A series of molecular dynamics simulation has been performed to study the structure of water-methanol and water-formamide mixtures. Besides the evaluation of partial radial distribution functions describing the hydrogen-bonded structure of the mixtures with different composition, the clustering properties and topology of hydrogen-bonded network were investigated as well (Fig. 4). The results have shown that these mixtures exhibit an extended structure in solution.

At low methanol concentration water molecules form a percolated network, methanol molecules are incorporated as monomers or short chains and together form a percolated

system. In methanol-rich mixtures short water chains and longer methanol chains build up the hydrogen-bonded clusters in the system. On the basis of the statistical analysis of configurations obtained from molecular dynamics simulation it has been found that more methanol molecules are connected to non-cyclic entities, while more water molecules form rings that might have been predicted on the basis of the stoichiometry of the mixtures. This finding can be explained by the presence of microscopic configurational inhomogeneity in water-methanol mixtures. In water-formamide mixtures the average hydrogen bonded neighbours number of molecules (water,formamide) and the the distribution of H-bonded neighbour does not change significantly as a function of formamide mole fraction. In these mixtures the molecules form percolated network in all concentration. It reveals on the basis of the same analysis, that the composition of cyclic entities in these system are very close to the ideal, thus so we find a microscopic homogeneity in this system. The calculated and measured total radial distribution function agreed very well with each other.

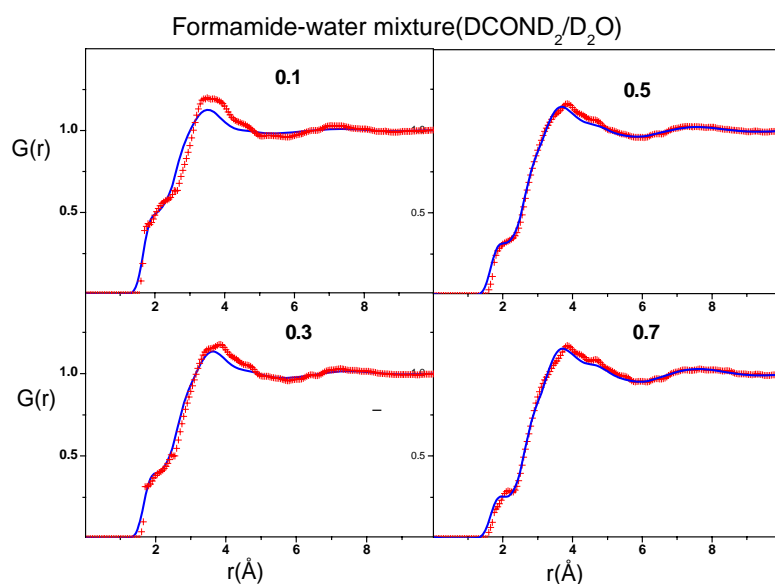
Figure 4. Representation of hydrogen bonded network in liquid methanol, water and formamide



We have also performed series of neutron diffraction experiment on DCOND2/D2O mixtures on 7C2 diffractometer in Saclay. We analysed these data using the MCGR program

developed by László Pusztai to avoid the Fourier cut off error. The calculated and measured total radial distribution functions agreed very well with each other. We show this on Fig 5.

Fig. 5. Total intermolecular radial distribution function from neutron diffraction experiment (Blue line: simulation, red cross: ND experiment)



1. **Bakó, I.**, Megyes, T., Bálint, S., Grósz, T., Chihaiia, V.: Water-methanol mixtures: Topology of hydrogen bonded network, *Phys. Chem. Chem. Phys.*, 2008, 10(32), 5004
2. **Bakó, I.**; Megyes, T.; Balint, S.; Chihaiia, V.; Bellissent-Funel, M.-C.; Krienke, H.; Kopf, A.; Suh, S. H.; Hydrogen bonded network properties in liquid formamide, *J. Chem. Phys.* 2010, 132(1), 014506
3. **Bakó I.**; Megyes, T.; Bálint, Sz.; Grósz, T. é Chihaiia, V.: Water-methanol Mixtures: Topology of Hydrogen Bonded Network, lecture, *Faraday Discussion* 141: Water - From Interfaces to the Bulk, Edinburgh, United Kingdom, 2008

4. **Imre Bakó**, Szabolcs Bálint, Tünde Megyes and Viorel Chihaiia Hydrogen bond network topology in aqueous solutions XVIII In. Conference on Horizons on Hydrogen bond research, 14-18 September 2009, Paris, France
5. **Imre Bakó**, Szabolcs Bálint, Tünde Megyes and Viorel Chihaiia H-bond network cooperativity in liquid water XIX. International Conference on "Horizons in Hydrogen Bond Research" 12-17 September Gottingen

6.

The nature of $\text{NO}_3\text{---H}_2\text{O}$ interactions in aqueous solutions and at interfaces is of prime importance in many fields including areas as diverse as atmospheric chemistry and nuclear waste. Nitrate ion is one of the most abundant ionic species in the atmosphere as well as in acidic wastes. Being present in atmospheric aerosols both in the polluted and remote troposphere, nitrate ions are involved in a variety of atmospheric chemical processes. For a long time, the hydration structure of the nitrate ion was an attractive subject in the solution chemistry.

The nitrate ion has been classified as the “order destroying” anion in hydrogen-bonded liquid water, owing to its large ionic size and relatively small charge. Thus, we have also studied the structure of NaNO_3 in water at different concentrations (1.88 M, 2.50 M, 5.63 M and 7.50 M).

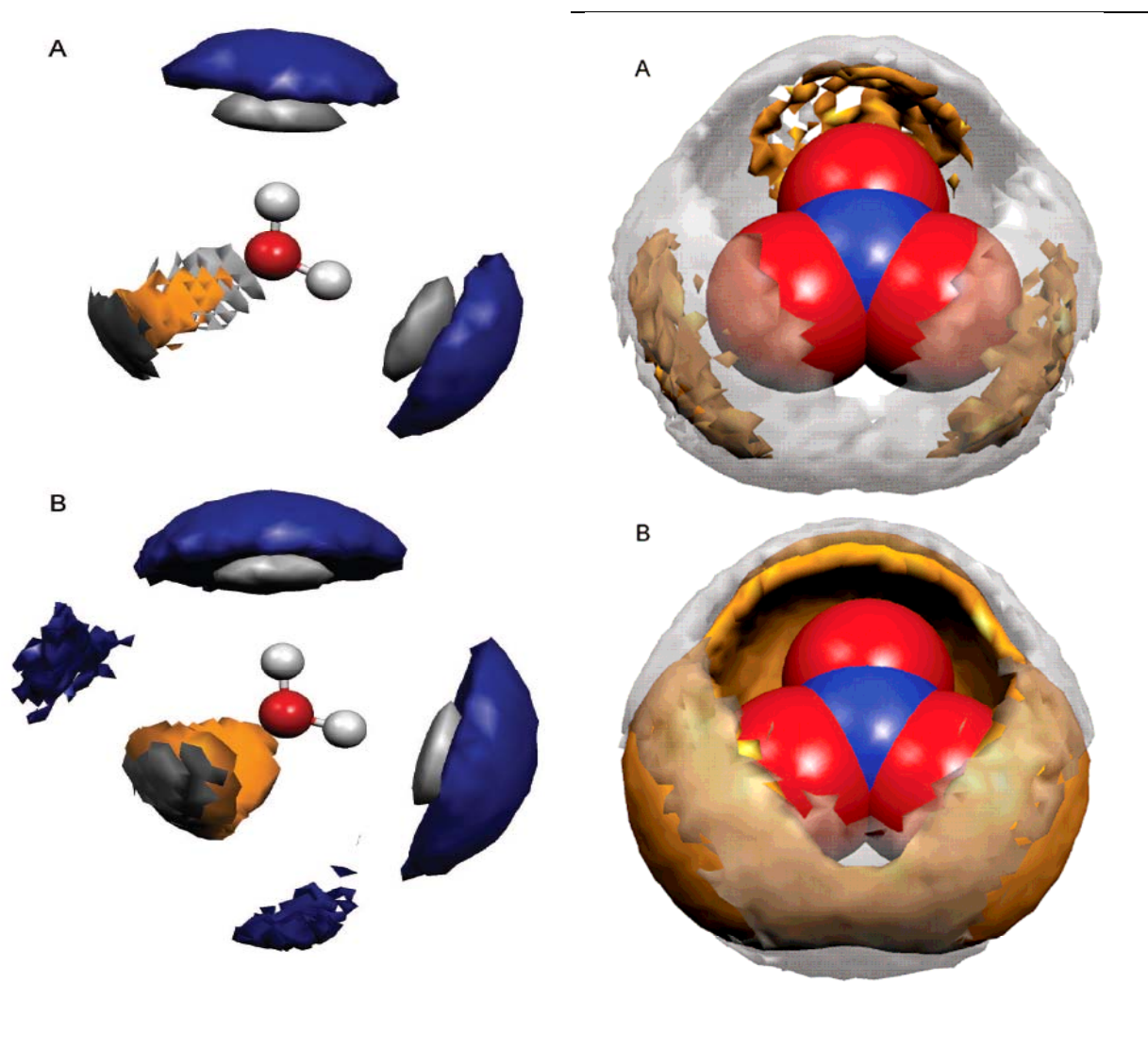
We performed a systematic work for NaNO_3 solutions in a wide concentration range using a joint diffraction and molecular dynamics study. Besides the evaluation of the solution structure, the limitations of the methods applied are discussed. The more detailed analysis of the partial RDFs casts a comprehensive and convincing picture about both sodium and nitrate ion solvation. The concentration effect of decreasing coordination numbers around sodium ions by increasing concentration is proven and even more, a building up of sodiumnitrate ion

pairs is demonstrated, which probably would not be possible to find out without simulation. Beyond the description of solvation structure of ions, a detailed analysis of disruption of “bulk” water structure could also be given - an often neglected area of studies.

Qualitative conclusions seem to be evident; hydrogen bonds of $Ow \cdots Ow$ types are breaking up and of $Ow \cdots ON$ types are building up.

The spatial distribution of water molecules and sodium ions around a central nitrate ion is presented on Figure 6. b (limits of ranges: $N \cdots Ow < 4.5 \text{ \AA}$ and $N \cdots Na < 4.5 \text{ \AA}$). The orange isosurface of probability identifies the regions where the sodium ions are likely found in the first sphere of nitrate ion, forming contact ion pairs. It can be clearly observed, that at high concentration the isosurface probability is denser supporting that the contact ion pair formation in highly concentrated solutions is more extended. Simultaneously, the gray marked probability isosurface of water becomes narrower indicating that with increase in concentration less water molecules are found in the hydration sphere of nitrate ion.

Figure 6. a) The spatial distribution of the ater (gray), sodium (yellow), and nitrate ions (blue) around a central water molecule for solutions A and B; b) the spatial distribution of the water (gray) and sodium ions (yellow) around a central nitrate ion, in the first hydration shell.



1. Megyes, T., Bálint, S., Peter, E., Grósz, T., **Bakó, I.**, Krienke, H., Bellissent-Funel, M. C.:
Solution structure of NaNO₃ in Water: Diffraction and molecular dynamics simulation study, J. Phys.
Chem. B, 2009, 113(13), 4054

2. Megyes, T.; Bálint, Sz.; Grósz, T.; Krienke, H.; Belissent-Funel, M. C.; **Bakó I.;** Solution
Structure of NaNO₃ in Water: Diffraction and Molecular Dynamics Simulation Study, lecture, ESF-
FWF Conference, International Workshop: Aqueous Solutions and their Interfaces, Heraklion, Crete,
Greece, 2008

7.

In the study of aqueous electrolyte solutions, alkali ion solutions are especially interesting due to their important role in solution chemistry, biochemistry, and pharmacology.

Knowledge of their solution structure is central to understand the transport properties of ions, the ionic permeability of organic structures such as biological membranes, and the efficacy of ions in precipitating, or salting out, proteins from aqueous solutions,

According to the literature data there is an uncertainty as far as hydration number of Na⁺ is concerned, placing it between 4 and 8 and the general concept of sodium being a “loosely hydrated” ion.. The diffuse character of literature data about the hydration of sodium ion is probably due to the chemical nature of the base as well as the experimental difficulties associated with these corrosive and viscous solutions

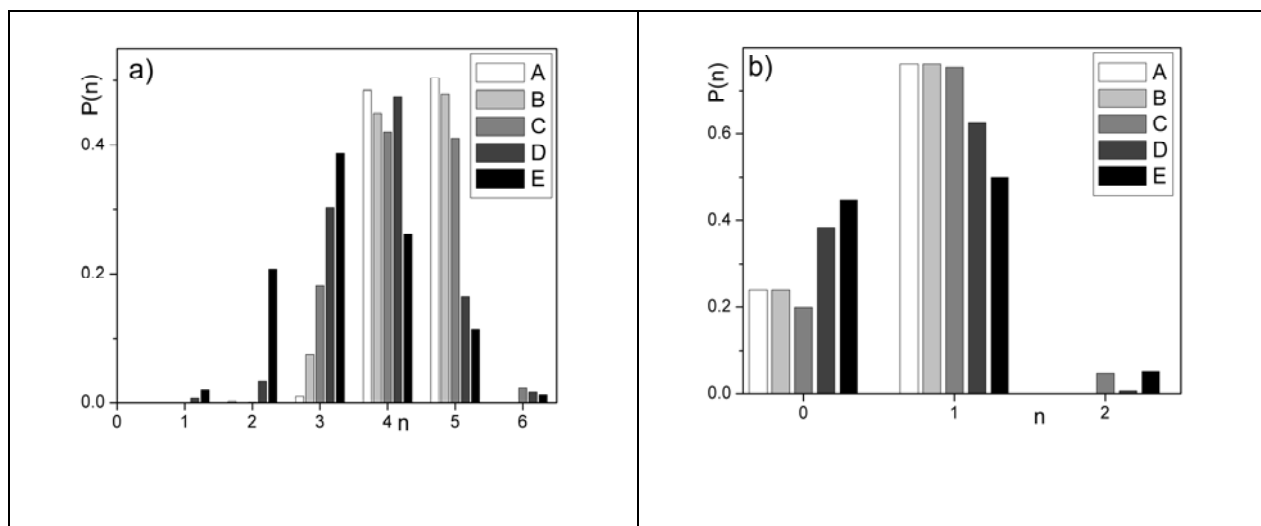
The solvation shell of OH⁻ in water is not composed any more of three accepted and one donated hydrogen bonds, as the standard Lewis picture of an isolated OH⁻ molecule would suggest. Recent ab initio molecular dynamic simulations suggest the oxygen of the hydroxide ion can accept up to four hydrogen bonds from surrounding water molecules to form a “hypercoordinated” H₅O₅⁻ - ion. The simulations also advocate that a breakage of a hydrogen bond to this four coordinate complex facilitates proton transfer because the two

oxygen atoms of a H_3O_2^- ion can each support up to three hydrogen bonds. These results are proved by the neutron diffraction experiment so the hydrated OH^- is mostly hypercoordinated²⁷ in the sense that its oxygen prefers to accept four hydrogen bonds in a roughly square-planar configuration. In addition, its hydrogen is able to donate another hydrogen bond

In this work a systematic work has been performed for NaOH solution of high concentration using x-ray diffraction. The results of diffraction experiments were compared to MD and CPMD simulations in order to obtain a more reliable picture of the structure of the liquids. Classical molecular dynamics simulations were not able to correctly describe the bulk structure of these solutions. However, Car-Parrinello simulation proved to be a suitable tool in the detailed interpretation of the hydration sphere of ions and bulk structure of solutions

The more detailed analysis of the partial radial distribution functions casts a comprehensive and convincing picture about both sodium and hydroxide ion solvations. The concentration effect of decreasing coordination numbers around sodium ions by increasing concentration is proven and even more, a building up of sodium hydroxide ion pairs is demonstrated and supported by CPMD simulation study. The hydroxide ion hydration is examined as well and, to the best of our knowledge, this is the first time when hypercoordination of hydroxide ions (figure 7) is supported by a joint x-ray diffraction and molecular dynamics simulation study.

Figure 7. Fraction of hydroxide ions with n water molecules in their solvation shells bounded by the oxygen atom a. and by the hydrogen atom b. of the hydroxide ion at various solute concentrations (A: 44 H₂O and 2 NaOH; B: 46 H₂O and 4 NaOH; C: 36 H₂O and 6 NaOH; D: 30 H₂O and 10 NaOH; E: 26 H₂O and 12 NaOH).



1. Vacha R., Megyes T., **Bako I.**, Pusztai L., Jungwirth P.:

Benchmarking polarizable molecular dynamics simulations of aqueous sodium hydroxide by diffraction measurements, *J. Phys. Chem. A*, 2009, 113(16), 4022

2. Megyes, T., Bálint, S., Grósz, T., Radnai, T., **Bakó, I.**, Sipos, P.: The structure of aqueous sodium hydroxide solutions: A combined solution x-ray diffraction and simulation study, *J. Chem. Phys.*, 2008, 128(4), 044501

7.

The solvation of ions in water plays an essential role in many chemical and biological as well as industrial systems. However, the structure of ionic solutions is not well understood, and from an experimental point of view it is difficult to obtain structural information.

Electronic polarizability and the charge transfer process is an important factor when we want to understand the electrostatic interactions between ion and water molecule. There are a significant interest to further investigate at a theoretical level the water polarization in the presence of a positive ion by investigating the electronic nature of such a process.

First-principle calculations based on DFT describe the electronic density using the Kohn-Sham orbitals, whose delocalised nature renders the assignment of atomic or molecular properties difficult. The concept of the maximally localised Wannier function provides a convenient framework to analyze atomic and molecular properties in the condensed phase. The centers of the maximally localized Wannier functions(MWFC) are used to localize, in the form of point charges, the electron density around single molecules, and the resulting molecular dipoles of several clusters and that of the first solvation shell of a standard liquid-ion system are compared and interpreted. It has already showed, that the dipole moment of water molecule in the first shell of Ca^{2+} , Mg^{2+} and Al^{3+} ion are significantly larger than the dipole moment of water in liquid.

In this work we performed series of optimisation of M-6wa (M: Na^+ , K^+ , Ca^{2+} , Mg^{2+} , Zn^{2+} , Al^{3+} , Ga^{3+}) complexes using BLYP-D3 method. Structural properties of these complexes agreed well with the results from high level ab initio calculation. We calculated the dipole moment of water around these ion using MWFC technique. We performed these calculation with and without ion in the center and substituting the ion with a corresponding charge. The results are presented on Table 1.

Table 1. The calculated dipole moment (Debye) of M-Wa system

	rMO	Dip1	Dip2	Dip1w	Dip4w
Na+	2.45	2.38	2.34	1.42	1.78
K+	2.85	2.26	2.17	1.67	1.79
Mg ²⁺	2.12	3.04	3.03	1.48	1.76
Zn ²⁺	2.13	3.32	2.99	1.48	1.79
Ca ²⁺	2.41	3.07	2.94	1.40	1.77
Ga ³⁺	2.03	4.32	3.91	1.38	1.77
Al ³⁺	1.945	4.05	4.03	1.38	1.73

rMO: M-O distance(Å), Dip1: M-6wa system (Debye), Dip2 M-6wa system from (M-6wa system optimized geometry put the corresponding charge in the place of ion), Dip1w 6water from M-6wa without ion, Dip4w one water molecule from M-6wa, M: cation

We can conclude from these calculation that the charge transfer process and the covalency between ion and water molecule play only a minor role for determining the dipole

moment of water in the first shell (Dip1 and Dip2 comparison). It is clear that the water-water repulsion in the first shell cause a significant reduction of dipole moment of water molecule.

The geometrical effect of water molecule on the dipole moment (Dip4w) is very small. IR, Raman measurements, and ab initio molecular dynamics simulations have been carried out to describe and understand the structural and dynamic behavior of hydrated Pt^{2+} ion in water. The experiments have revealed strong red-shifted O–H bond frequencies and blue-shifted ligand deformation bands. The simulations have showed that the presence of the doubly charged cation and the enhanced hydrogen bond formations between the first and second shells result in significant structural changes in the first solvation shell, which in turn yield the characteristic shifts in the vibrational spectra

1. Stirling, A., Bakó, I., Kocsis, L., Hajba, L., Mink, J.: Pt(II)-ion hydration: Structural and vibrational characteristics from theory and experiment, *Int. J. Quant. Chem.* 2009, 109(11), 2591

Reference:

- [ⁱ] O. Rodriguez de la Fuente, M. Borasio, P. Galletto, G. Rupprechter and H. J. Freund, *Surf. Sci.* 566 – 568 (2004) 740.
- [ⁱⁱ] M. Morkel, V. V. Kaichev, G. Rupprechter, H. J. Freund, I. P. Prosvirin and V. I. Bukhtiyarov, *J. Phys. Chem. B* 108 (2004) 12955.
- [ⁱⁱⁱ] J. -J. Chen, Z. -C. Jiang, Y. Zhou, B. R. Chakraborty and N. Winograd, *Surf. Sci.* 328 (1995) 248.
- [^{iv}] M. Rebholz and N. Kruse, *J. Chem. Phys.* 95 (1991) 7745.
- [^v] M. Mavrikakis and M. Barteau, *J. Molec. Catal. A* 131 (1998) 135.
- [^{vi}] R. Schennach, A. Eichler and K. D. Rendulic, *J. Phys. Chem B*, 107 (2003) 2552.
- [^{vii}] R. Schennach, G. Krenn and K. D. Rendulic, *Vacuum*, 71 (1-2) (2003) 89.
- [^{viii}] R. Schennach, G. Krenn, B. Klötzer and K. D. Rendulic, *Surf. Sci.* 540 (2-3) (2003) 237.
- [^{ix}] G. Krenn and R. Schennach, *J. Chem. Phys.* 120 (12) (2004) 5729.
- [^x] G. Krenn, H. P. Koch and R. Schennach, *Vacuum*, 80 (1-3) (2005) 40.
- [^{xi}] H. P. Koch, G. Krenn, I. Bako and R. Schennach, *J. Chem. Phys.* 122 (24) (2005) 244720.
- [^{xii}] J. E. Parmeter, X. Jiang, and D. W. Goodman, *J. Vac. Sci. Technol. A* 9 (3) (1991) 1810.
- [^{xiii}] F. Solymosi, T. I. Tarnóczy and A. Berkó, *J. Phys. Chem.* 88 (1984) 6170.
- [^{xiv}] Y. Suwa, S. -I. Ito, S. Kameoka, K. Tomishige and K. Kunimori, *Appl. Catal. A* 267 (2004) 9.
- [^{xv}] T. Shishido, H. Sameshima and K. Takehira, *Topics in Catal.* 22 (3-4) (2003) 261.
- [^{xvi}] N. Iwasa, S. Masuda, N. Ogawa and N. Takezawa, *Appl. Catal. A* 125 (1995) 145.
- [^{xvii}] N. Iwasa, T. Mayanagi, W. Nomura, M. Arai and N. Takezawa, *Appl. Catal. A* 248 (2003) 153.
- [^{xviii}] C. -H. Kim, J. S. Lee and D. L. Trimm *Topics in Catal.* 22 (3-4) (2003) 319.
- [^{xix}] N. Iwasa, H. Suzuki, M. Terashita, M. Arai and N. Takezawa, *Catal. Lett.* 96 (1-2) (2004) 75.
- [^{xx}] P. M. Jones, J. A. May, J. B. Reitz and E. I. Solomon, *J. Am. Chem. Soc.* 120 (1998) 1506.
- [^{xxi}] A. Y. Rozovskii and G. I. Lin, *Topics in Catal.* 22 (3-4) (2003) 137.
- [^{xxii}] J. Nakamura, Y. Choi and T. Fujitani, *Topics in Catal.* 22 (3-4) (2003) 277.
- [^{xxiii}] T. Fujitani and J. Nakamura, *Appl. Catal. A* 191 (2000) 111.
- [^{xxiv}] M. Kurtz, J. Strunk, O. Hinrichsen, M. Muhler, K. Fink, B. Meyer and C. Wöll, *Angew. Chem. Int. Ed.* 44 (2005) 2790.
- [^{xxv}] K. M. Neyman, R. Sahnoun, C. Inntam, S. Hengrasmee and N. Rösch, *J. Phys. Chem. B* 108 (2004) 5424.
- [^{xxvi}] Z. -X. Chen, K. M. Neyman and N. Rösch, *Surf. Sci.* 548 (2004) 291.
- [^{xxvii}] Z. -X. Chen, K. M. Neyman, K. H. Lim and N. Rösch, *Langmuir* 20 (2004) 8068.
- ^{xxviii} G. Kresse and J. Hafner, *Phys. Rev. B* **47** C558 (1993).

